Journal of Pharmaceutical Analysis 6 (2016) 165–170

HOSTED BY

Contents lists available at ScienceDirect

Journal of Pharmaceutical Analysis

journal homepage: www.elsevier.com/locate/jpa
www.sciencedirect.com

Original Article

Molecular dynamics of amorphous pharmaceutical fenofibrate studied by broadband dielectric spectroscopy ☆

U. Sailaja [a,*], M. Shahin Thayyil [b], N.S. Krishna Kumar [c], G. Govindaraj [c]

[a] Department of Physics, M.E.S Keveeyam College, Valanchery, 676552 Malappuram, Kerala, India
[b] Department of Physics, University of Calicut, 673635 Kerala, India
[c] Department of Physics, School of Physical, Chemical and Applied Sciences, Pondicherry University, Puducherry 605014, India

ARTICLE INFO

Article history:
Received 12 February 2014
Received in revised form
1 September 2014
Accepted 4 September 2014
Available online 16 September 2014

Keywords:
Amorphous fenofibrate
Bioavailability
Broadband dielectric spectroscopy
Glass transition
Molecular dynamics

ABSTRACT

Fenofibrate is mainly used to reduce cholesterol level in patients at risk of cardiovascular disease. Thermal transition study with the help of differential scanning calorimetry (DSC) shows that the aforesaid active pharmaceutical ingredient (API) is a good glass former. Based on our DSC study, the molecular dynamics of this API has been carried out by broadband dielectric spectroscopy (BDS) covering wide temperature and frequency ranges. Dielectric measurements of amorphous fenofibrate were performed after its vitrification by fast cooling from a few degrees above the melting point (T_m=354.11 K) to deep glassy state. The sample does not show any crystallization tendency during cooling and reaches the glassy state. The temperature dependence of the structural relaxation has been fitted by single Vogel–Fulcher–Tamman (VFT) equation. From VFT fit, glass transition temperature (T_g) was estimated as 250.56 K and fragility (m) was determined as 94.02. This drug is classified as a fragile glass former. Deviations of experimental data from Kohlrausch–Williams–Watts (KWW) fits on high-frequency flank of α-peak indicate the presence of an excess wing in fenofibrate. Based on Ngai's coupling model, we identified the excess wing as true Johari–Goldstein (JG) process. Below the glass transition temperature one can clearly see a secondary relaxation (γ) with an activation energy of 32.67 kJ/mol.

1. Introduction

To increase the solubility and bioavailability of the poorly water soluble crystalline drugs is a challenge to modern pharmaceutical scientists. One of the promising methods for improving solubility and bioavailability of poorly water soluble crystalline drugs is to prepare them in the amorphous form. Amorphous form of pharmacologically active materials is very important because this form has enhanced thermodynamic properties, having high internal energy, solubility, bioavailability, dissolution rate, better compression characteristics and greater therapeutic activity than the corresponding crystalline counterpart [1–4]. However, amorphous systems are physically and chemically unstable and therefore show crystallization tendencies.

Recent studies on various amorphous pharmaceutical drugs show that molecular mobility above and below the glass transition temperature (T_g) plays an important role in the devitrification of the drugs. The knowledge about the molecular dynamics of the drugs in the amorphous phase is very important for safety storage in order to obtain the maximum shelf-life and stability [5–8].

Fenofibrate had been chosen as a model drug for the current study. It is a fibric acid derivative which has greater high density lipoprotein cholesterol (HDL-CH) rising and greater low density lipoprotein cholesterol (LDL-CH) lowering action than other fibrates [9]. To the best of our knowledge, this will be the first attempt to describe the dielectric relaxation study of amorphous fenofibrate.

For this it is essential to have a better understanding of molecular dynamics in supercooled and glassy state of this API. In the present study, we used differential scanning calorimetry (DSC) for thermal transition analysis and observed that fenofibrate is a very good glass former. Based on DSC study, dielectric measurements of this API were carried out by broadband dielectric spectroscopy (BDS) as an investigative tool to study the molecular dynamics of amorphous systems in a wide range of frequencies ($f=10^9$–10^{-2} Hz) at different thermodynamic conditions (P, T). Recently this technique has been successfully applied to study the molecular dynamics of various amorphous pharmaceuticals [10–12]. To get a clear picture of hydrogen bonding in the crystalline and amorphous state of fenofibrate, infrared (IR) spectroscopy was used.

☆Peer review under responsibility of Xi'an Jiaotong University.

* Corresponding author. Tel.: +91 9400846070.
E-mail address: sailajaurpayil@gmail.com (U. Sailaja).

http://dx.doi.org/10.1016/j.jpha.2014.09.003

2. Material and methods

2.1. Material

Fenofibrate, a white crystalline powder CAS no. 6271-86-2, was supplied by Sigma Aldrich with purity ≥99%. The drug was crystalline in nature as confirmed by the sharp diffraction patterns of the PXRD result, which is depicted in Fig. 1. Its chemical structure is presented in Fig. 2. Obtained material was used as received without further purification.

2.2. Methods

2.2.1. Image analysis system (IAS)

Image analysis was used to investigate micro- and macro-specimens objectively to provide information regarding the microstructure, quantity, size, area, shape and phase analysis. Images were captured using light optical microscope and analyzed using image analysis software. This technique can be applied in the field of material science, biological science, pharmaceutical science, etc. Particle size of fenofibrate was taken by dispersing the sample in water.

2.2.2. DSC

A DSC instrument (821^e Mettler-Toledo GmbH) operated with STAR^e software version 9.1 and equipped with an intracooler was used for the thermal transition studies. The instrument was calibrated by using indium for temperature and specific heat. Fenofibrate of 3.1540 mg was analyzed under dry nitrogen purge (50 mL/min) in a sealed pinhole aluminum pan. The sample was heated from room temperature to 91 °C and held for 3 min; it was cooled to −50 °C and held for 5 min; and again it was heated to 91 °C. During the entire process a constant heating and cooling rate of 10 °C/min was used. Thermograms were collected during heating. Melting point (T_m) was determined as the onset of the endothermic peak, whereas glass transition temperature (T_g) was measured as the onset of the glass transition.

2.2.3. Fourier transform infrared (FTIR) spectroscopy

The IR spectra of crystalline and amorphous samples were collected on a Perkin Elmer (model: Synthesis Monitoring System) and Nicolet instruments corporation USA (Model MAGNA), respectively.

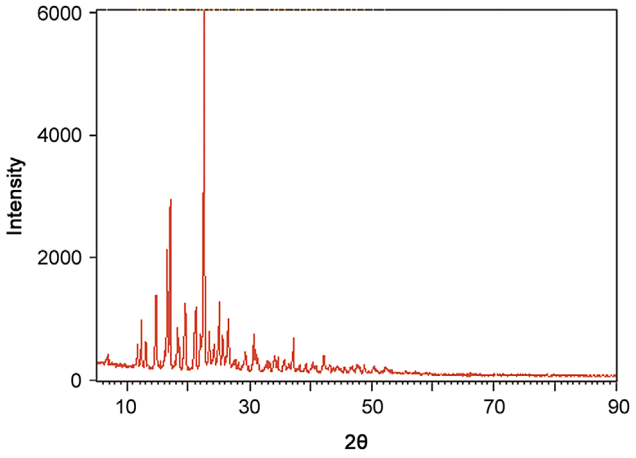

Fig. 1. XRPD pattern of crystalline fenofibrate.

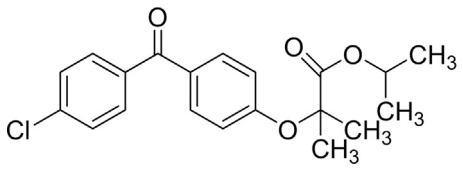

Fig. 2. The chemical structure of fenofibrate.

2.2.4. BDS

Isobaric dielectric measurements at ambient pressure were carried out using Novo-Control GMBH alpha dielectric spectrometer covering a frequency range from 10^{-2} to 10^7 Hz. Temperature was controlled by using a nitrogen gas cryostat with temperature stability better than 0.1 K. The tested sample was placed in a measurement capacitor made of stainless steel (diameter: 30 mm, gap: 0.20 mm). Teflon was used as the spacer. Dielectric measurements of fenofibrate were performed after its vitrification by fast cooling (10 K/min) from a few degrees above the melting point (T_m=354.11 K). The temperature measurements were carried out from 123.15 K to 305.15 K in different steps. However, the sample did not crystallize during cooling from the melting temperature.

3. Results and discussion

3.1. Particle size

Particle size of fenofibrate was analyzed by IAS and the maximum size was found to be 9.95 μm and the minimum was found to be 1.91 μm. The details of analysis are presented in Table 1.

3.2. Thermal studies

The onset glass transition was observed at 254.15 K, which is considered as the glass transition temperature (T_g) of fenofibrate. The onset melting of the sample was observed at 354.11 K, which is melting temperature (T_m) of the sample. No crystallization was observed either cooling below T_g or subsequent heating up to melting point. These results were in good agreement with those reported by Baird et al. [13] and Zhou et al. [7]. Thermodynamic quantities obtained from the current work and from the literature are listed in Table 2. The obtained thermogram of fenofibrate is presented in Fig. 3.

3.3. Spectroscopic investigation of hydrogen bonding

The spectra of fenofibrate showed different strengths of hydrogen bonding (Fig. 4A and B). Two carbonyl peaks were seen in the crystalline and amorphous fenofibrate, one from the C=O, and the other from the methyl ester carbonyl group. Crystalline fenofibrate showed two peaks at 1729.53 cm^{-1} and 1651.48 cm^{-1}, respectively. But in the amorphous form two peaks were seen at 1728.25 cm^{-1} and 1654.22 cm^{-1}, respectively. Because of the hydrogen bond formation the carbonyl peak position shifted to a lower wave number. In the amorphous phase, only one carbonyl group took part in the hydrogen bond formation by a downward shift of 1.28 cm^{-1}. The other peak shifted by value of 2.74 cm^{-1} to a higher peak position. The upward shifted in the position of the C=O group suggests that the hydrogen bond in the crystalline

Table 1
Class interval and number of particles of fenofibrate.

ID class	Class interval (μm)	No. of particles
1	0–2	280
2	2–4	777
3	4–6	371
4	6–8	163
5	8–10	79
6	10–12	0

phase is stronger than that in the amorphous phase. In addition to the above groups capable of classical hydrogen bond formation, the stretching frequencies of the CH_3 were investigated in both the phases [14,15].

3.4. Molecular dynamics

Dielectric loss spectra (i.e., imaginary part of dielectric permittivity ε'' plotted as a function of frequency f) of fenofibrate is shown in Fig. 5. Fig. 5A shows the primitive relaxation process measured above T_g. T_g is defined as the temperature at which the structural relaxation time (τ_α) approaches a value of 100 s. Dielectric loss spectra collected above T_g exhibited the most intense relaxation i.e., α-relaxation (originating from cooperative reorientational motion of molecules) along with conductivity. The strength of the dielectric spectra started decreasing from 289.15 K onwards, indicating that fenofibrate started crystallizing. Fig. 5B shows the secondary relaxation present below T_g of this sample. The decrease in dipoles due to crystallization was also observed from the real part of the permittivity (Fig. 6). Both ε' and ε'' were analyzed by using the Win FIT V (3.2) software. The dielectric spectra were fitted by using the Havriliak–Negami (HN) function as given below

$$\varepsilon^*(\omega) = \varepsilon' - i\varepsilon'' = \left[\varepsilon_\infty + \sum_k \left(\frac{\Delta\varepsilon}{(1 + (i\omega\tau_{HNk})^{\alpha_{HNk}})^{\beta_{HNk}}}\right)\right] \quad (1)$$

where k sums over different relaxation processes, ω is the angular frequency, τ_{HN} is the characteristic relaxation time which is related to the frequency of maximal loss f_{max}, $\Delta\varepsilon$ is the dielectric strength, ε_∞ is the high frequency limit of the real part $\varepsilon'(\omega)$; α_{HN} and β_{HN} are the symmetric and asymmetric broadenings of loss curve. For the secondary relaxation process, $\beta_{HN}=1$, then HN function becomes the Cole–Cole function.

Table 2
Thermodynamic quantities during melting and glass transition of fenofibrate.

Compound	MW (g/mol)	T_m (K)	T_g (K)	Ref.
Fenofibrate	360.83	354.11	254.15	This work
		354.15	254.15	[13]
		353.65	253.15	[7]

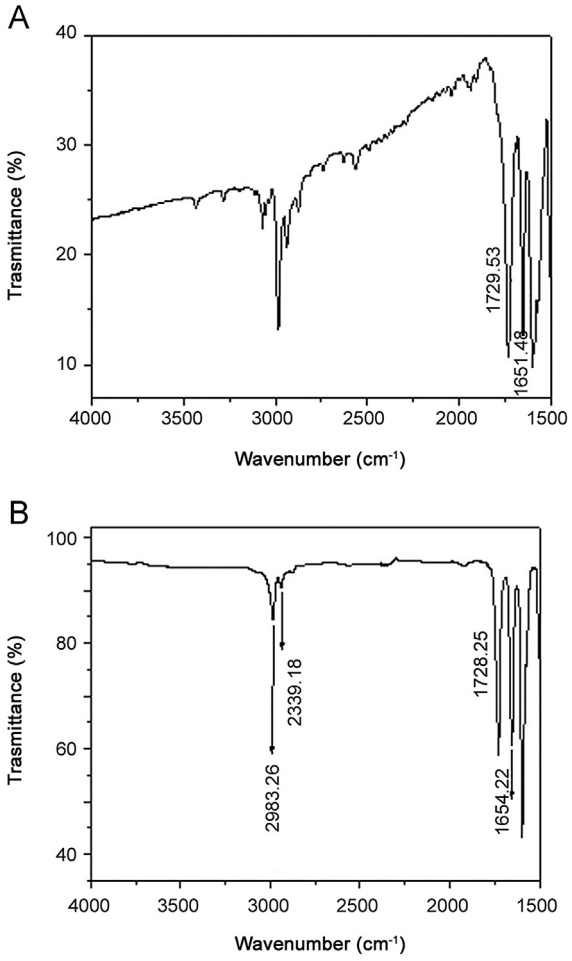

Fig. 4. Spectral variations of fenofibrate in C═O stretching vibration region. (A) crystalline fenofibrate and (B) amorphous fenofibrate.

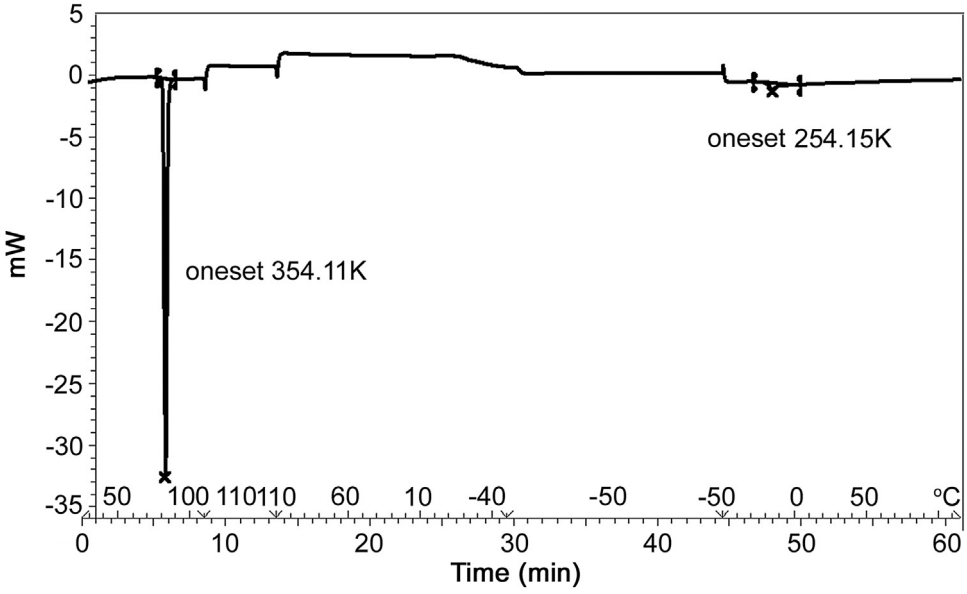

Fig. 3. DSC thermogram of fenofibrate obtained during heating/cooling with 10 °C/min. Heating of the sample yields T_m=354.11 K as the onset melting temperature. Subsequent cooling of the melt from 364.15 K down to 223.15 K. Following heating of the vitrified fenofibrate to a temperature higher than T_m (364.15 K). The onset glass transition temperature (T_g) obtained on heating is 254.15 K: at higher temperature there is no evidence of crystallization.

In order to check the presence of true secondary relaxation coming from the intermolecular motion called Johari–Goldstein (JG) or (β) relaxation in fenofibrate, coupling model (CM) prediction was applied [16,17]. According to this theoretical tool there is a good agreement between the JG-relaxation time (τ_{JG}) and the primitive relaxation time (τ_0) calculated from Eq. (2)

$$\tau_{JG}(T) \cong \tau_0(T) = (t_c)^n(\tau_\alpha(T))^{1-n} \quad (2)$$

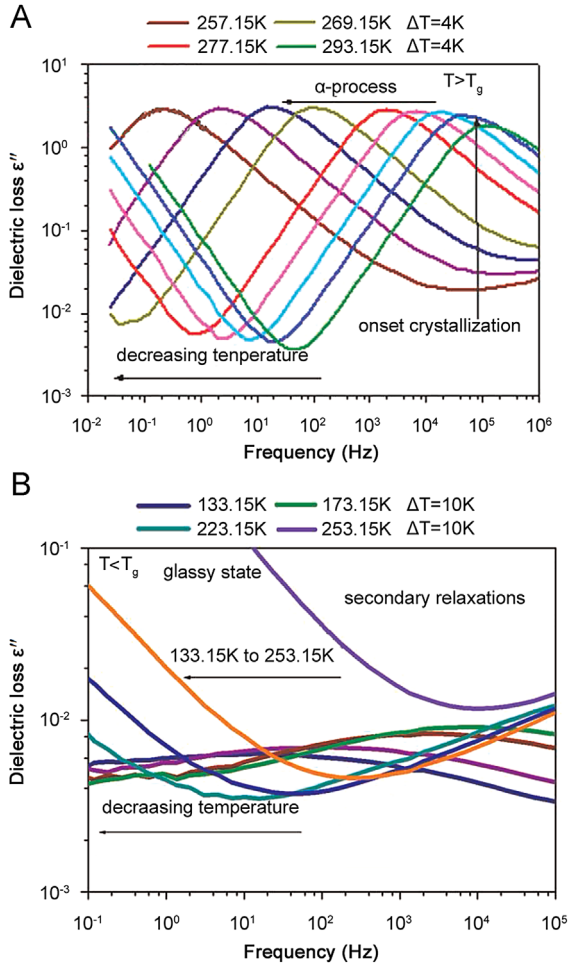

Fig. 5. Dielectric loss curves obtained for fenofibrate during heating. (A) the primary relaxation above T_g and (B) the secondary relaxation below T_g.

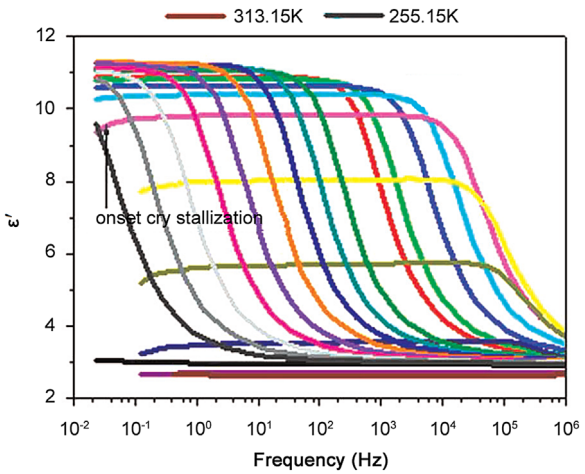

Fig. 6. Variation of real part of the complex permittivity for fenofibrate with temperature at different frequencies.

where $n=(1-\beta_{KWW})$ is the coupling parameter, t_c is the crossover time which represents the crossover from independent to co-operative motions and equal to 2 ps for small molecular glass formers.

To describe the non-exponential behavior of α-relaxation the one-sided Fourier transform of KWW function was also used as given below

$$\phi(t) = \exp\left[-(t/\tau_{KWW})^{\beta_{KWW}}\right] \quad (3)$$

In the frequency domain, the parameter β_{KWW} describes the shape of the spectra. If $\beta_{KWW}=1$, it denotes symmetric and narrow relaxation peak, value of $\beta_{KWW}=0$ indicates very broad and asymmetric peak. For fenofibrate the procedure of fitting the α-peak by one-side Fourier transform of stretched exponential function at 257.15 K gives the value of $\beta_{KWW}=0.70$. This means that experimentally observed structural relaxation peak is asymmetric and broader than that of classical Debye response. This indicates the presence of an excess wing (EW). EW is a submerged process in which true secondary relaxation coming from the intermolecular motion is hidden under the prominent α-peak.

For fenofibrate, the value of $\tau_0=2.643\times10^{-4}$ s at $T=257.15$ K, corresponds to a frequency of $f_0=602.55$ Hz. Where f_0 is the primitive relaxation frequency ($f_0 = 1/2\pi\tau_0$) and it was found that f_0 was far from the maximum of secondary γ-relaxation peak and lay within the prominent structural relaxation peak. It clearly indicates that the secondary relaxation β (JG) which is a precursor of the α-relaxation and originating from the intermolecular motions is hidden under the prominent structural α-peak, which means that the well resolved γ-relaxation is non-JG secondary relaxation. Many investigations showed that high pressure measurements [18–21] as well as physical ageing [22,23] can separate the α-peak and EW.

The master curve was constructed in the following way. Several spectra above T_g were shifted horizontally to superimpose with that obtained at 257.15 K as shown in Fig. 7. The exponents α_{HN} and β_{HN} show constant value, i.e., $\alpha_{HN}\approx0.98$; $\beta_{HN}\approx0.57$, which indicates that the shape of the α-peak of fenofibrate does not change in that region.

Shamblin et al. [24] have suggested that the stretching parameter β_{KWW} has a very important role in predicting the stability of amorphous pharmaceuticals against crystallization. As β_{KWW} decreases (the asymmetric distribution of relaxation times becomes broader) stability would also decrease. By comparing the value of β_{KWW} of fenofibrate with other APIs (acetaminophen $\beta_{KWW}=0.79$

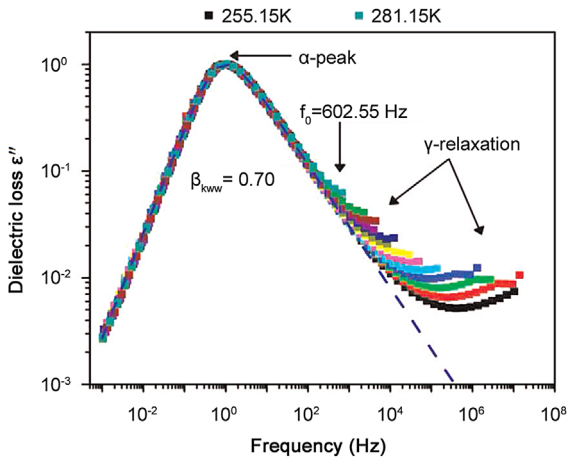

Fig. 7. Super imposed spectra of fenofibrate formed by shifting several spectra [255.15–281.15 K, $\Delta T=2$ K] above T_g to overlap the spectrum at 257.15 K. The KWW fit of the α-peak at 257.15 K yields $\beta_{KWW}=0.70$. The black arrow denotes the position of primitive relaxation frequency (f_0) calculated at 257.15 K using CM predictions.

[12], Nonivamide $\beta_{KWW}=0.79$ [25], Glibenclamide $\beta_{KWW}=0.74$ [26], Indapamide $\beta_{KWW}=0.72$ [27], and Ketoprofen $\beta_{KWW}=0.71$ [10]) according to the Shamblin criterion, it was found that stability of amorphous fenofibrate was lower than that of ketoprofen.

The observed secondary (γ-) relaxation probably originated from the intramolecular motion of small part of the fenofibrate molecule (local motions originating from the molecular fluctuations of methyl group). In FTIR spectrum (Fig. 5B) two distinct bands occurred at 2983.26 and 2939.18 cm^{-1}. The first band corresponded to asymmetrical stretching mode of C–H bonds of methyl group and the second band arose from the symmetrical stretching of C–H bonds.

The temperature evolution of the structural relaxation time τ_α very often follows the time honored Vogel–Fulcher–Tamman (VFT) expression, given as below

$$<\tau> = \tau_{VF} e^{B/|T-T_0|} \quad (4)$$

with τ_{VF}, B, and T_0 as parameters.

From VFT fit, we calculated the fragility "m" of fenofibrate by using Eq. (5):

$$m = \frac{d\log_{10}\tau_\alpha}{d\left(\frac{T_g}{T}\right)}/T = T_g \quad (5)$$

VFT fit reveals the value of T_g as 250.56 K. T_g obtained from VFT fit is in close agreement with that of our DSC study as well as that of the DSC study done by Baird et al. [13] and Zhou et al. [7]. The non-Arrhenius behavior of the α-peak gives the measure of the fragility parameter [28,29]. Strong systems have fragility less than 40 and fragile systems have fragility greater than 75 [1]. Fragile glass formers are physically unstable compared with the strong one. Fragility "m" in the case of fenofibrate was estimated as 94.02 and classified this API as a fragile glass former. Recent studies on ketoprofen by Shibata et al. [32] showed that there is a strong correlation between the fragility, boson peak frequency and shear modulus; large value of fragility is related to weak boson peak (or lower boson peak frequency which is caused by small shear modulus). So fragility is a very important parameter, which gives an insight to the theory of liquid–glass transition [30]. The strength parameter D was estimated as 7.04 proving fenofibrate as a fragile glass former. (T_g–T_o) was found to be 41.24, and T_m/T_g was found to be 1.4, and both the methods showed this API belongs to fragile group. The value of T_0 was obtained as 209.32 K. The temperature T_0 is often referred to as the Kauzmann temperature T_K, a hypothetical temperature where configurational entropy of supercooled liquid would be equal to entropy of the crystal and molecular mobility would reduce to the same level as that of the crystal (strictly speaking the molecular mobility is not zero). For most of the glassy systems, it lies between 50 and 70 K, below T_g and it is sufficient to ensure safety storage [4]. Recently Pajula et al. [31,32] have showed that the stabilization of amorphous drugs can be achieved by the addition of small molecular weight excipients.

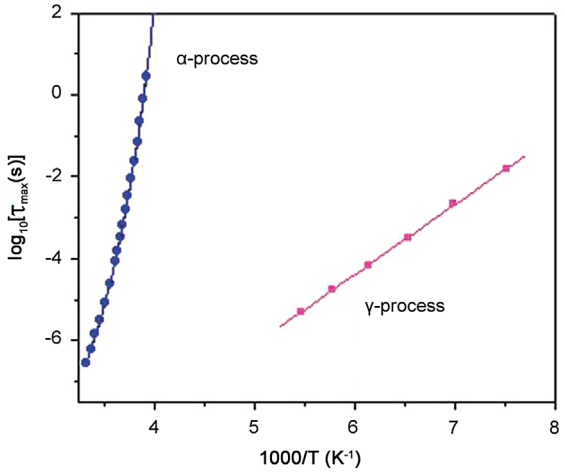

Fig. 8. Arrhenius plot of fenofibrate. Filled circles denote α-relaxation, while filled squares are for γ-relaxation. The solid lines are fit to the dielectric data using VFT form for α-process, and Arrhenius equation for γ-process.

Now we would like to discuss the secondary relaxation coming from the small part of the fenofibrate molecule which is the gamma relaxation. The temperature dependence of the relaxation time of the γ-process shows a linear dependence and can be described by the Arrhenius equation

$$\tau = \tau_\infty \exp[E_a/RT] \quad (6)$$

where τ_∞ is constant and E_a is the activation energy. The activation energy for fenofibrate was calculated and obtained as 32.67 kJ/mol. Fig. 8 shows the relaxation map of fenofibrate. The fitting parameters of VFT and Arrhenius equations are presented in Table 3.

4. Conclusions

The molecular dynamics of fenofibrate in the glassy and supercooled states was studied by different experimental techniques. Based on the study of the molecular dynamics of fenofibrate in the glassy and supercooled states by BDS, we are summarising the important results. Our measurements during cooling with a cooling rate of 10 K/min from the melt to deep glassy state do not show any crystallization tendency in fenofibrate, thereby showing their excellent glass forming ability. Fenofibrate shows structural (α) relaxation above T_g and one secondary relaxation process below T_g which is characterized as γ-relaxation.

The temperature dependence of α-relaxation times was described by single Vogel–Fulcher–Tamman equation. From VFT fits the glass transition temperature T_g was estimated as 250.56 K. T_g values calculated from dielectric measurements were found to be in good agreement with those measured from our DSC experiments as well as with the literature values.

Fragility represents the deviation from the Arrhenius behavior. It was obtained as 94.02 and we classified this API as a fragile glass former. T_0 was obtained as 209.32 K. So it is suggested that this API can provide a shelf life of at least 3–5 years when it is stored in freezer at a temperature less than T_0.

Application of the CM prediction indicated that the Johari–Goldstein (JG) relaxation is hidden under the prominent structural

Table 3
The fitting parameters for the VFT and Arrhenius equations of fenofibrate.

α-Process, VFT			γ-Process, Arrhenius			
T_0 (K)	log τ_{VF}	D	log $\tau_{\infty,\gamma}$	$E\gamma$ (kJ/mol)	m	T_g (K) (BDS)
209.32 ± 1.02	−13.52 ± 0.17	7.04 ± 0.20	−14.63 ± 0.09	32.67 ± 0.01	94.02	250.56

relaxation and manifested as an excess wing. The observed secondary relaxation is characterized as non-JG relaxation (γ relaxation) and assumed to be originated from the intramolecular degrees of freedom. The γ-relaxation has an Arrhenius temperature dependence and the activation energy is found to be $E_\gamma = 32.67$ kJ/mol. This drug shows crystallization tendency from 289.15 K onwards during heating in the dielectric measurements by BDS. The existence of intermolecular hydrogen bonding was verified by IR spectroscopy.

Acknowledgments

The authors gratefully acknowledge IIT Powai, Mumbai (India), CIL, NIPER, Mohali, (India) for providing experimental facilities. Sailaja acknowledges University Grants Commission (No. F.FIP/11th Plan/KLCA046TF, dated 12. May, 2009), Government of India for the award of a research fellowship under the Faculty Improvement Program (FIP).

References

[1] L. Yu, Amorphous pharmaceutical solids: preparation, characterization and stabilization, Adv. Drug Deliv. Rev. 48 (2001) 27–42.
[2] B.C. Hancock, M. Parks, What is the true solubility advantage for amorphous pharmaceuticals? Pharm. Res. 17 (2000) 397–404.
[3] P. Gupta, G. Chawla, A.K. Bansal, Physical stability and solubility advantage from amorphous celecoxib: the role of thermodynamic quantities ad molecular mobility, Mol. Pharm. 1 (2004) 406–413.
[4] B.C. Hancock, G. Zografi, Characteristics and significance of the amorphous state in pharmaceutical systems, J. Pharm. Sci. 86 (1997) 1–12.
[5] N.T. Correia, J.J. Moura Ramos, M. Descamps, et al., Molecular mobility and fragility in indomethacin: a thermally stimulated depolarization current study, Pharm. Res. 18 (2001) 1767–1774.
[6] Y. Aso, S. Yoshioka, S. Kojima, Relationship between the crystallization rates of amorphous nifedipine, phenobarbital, and flopropione, and their molecular mobility as measured by their enthalpy relaxation and ^{1}H NMR relaxation times, J. Pharm. Sci. 89 (2000) 408–416.
[7] D. Zhou, G.G.Z. Zhang, D. Law, et al., Physical stability of amorphous pharmaceuticals: Importance of configurational thermodynamic quantities and molecular mobility, J. Pharm. Sci. 91 (2002) 1863–1872.
[8] C. Bhugra, M.J. Pikal, Role of thermodynamic, molecular, and kinetic factors in crystallization from the amorphous state, J. Pharm. Sci. 97 (2008) 1329–1349.
[9] K.D. Tripathi, Essentials of Medical Pharmacology, Jaypee Brother's Medical Publications (P) Ltd., New Delhi, India, 2008, pp. 483.
[10] U. Sailaja, M. Shahin Thayyil, N.S. Krishna Kumar, et al., Molecular dynamics in liquid and glassy states of non-steroidal anti-inflammatory drug: ketoprofen, Eur. J. Pharm. Sci. 49 (2013) 333–340.
[11] A.R. Bra's, J.P. Noronha, A.M.M. Antunesn, et al., Molecular motions in amorphous ibuprofen as studied by dielectric spectroscopy, J. Phys. Chem. 112 (2008) 11087–11099.
[12] G.P. Johari, M. Kim, S. Shanker, Dielectric studies of molecular motions in amorphous solid and ultra viscous acetaminophen, J. Pharm. Sci. 94 (2005) 2207–2223.
[13] J.A. Baird, B.V. Eerdenbrugh, L.S. Taylor, A classification system to assess the crystallization tendency of organic molecules from under cooled melts, J. Pharm. Sci. 99 (2010) 3787–3806.
[14] X.C. Tang, M.J. Pikal, L.S. Taylor, Spectroscopic investigations of hydrogen bond patterns in crystalline and amorphous phases in dihydropyridine calcium channel blockers, Pharm. Res. 19 (2002) 477–483.
[15] R.M. Silverstein, G.C. Bassler, T.C. Morrill, Spectrometric Identification of Organic Compounds, fifth edition,. John Wiley&Sons, Singapore, 1991.
[16] K.L. Ngai, Correlation between the secondary β-relaxation time at T_g and the Kohlrausch exponent of the primary α-relaxation, Physica A 261 (1998) 36–50.
[17] K.L. Ngai, An extended coupling model description of the evolution of dynamics with time in supercooled liquids and ionic conductors, J. Phys. Condens. Matter 15 (2003) S1107–S1125.
[18] K. Kaminski, S. Maslanka, J. Ziolo, et al., Dielectric relaxation of α-tocopherol acetate (vitamin E), Phys. Rev. E 75 (2007) 0119031–0119037.
[19] Z. Wojnarowska, K. Adrjanowicz, K. Kaminski, et al., Effect of pressure on tautomers equilibrium in super cooled glibenclamide drug, analysis of fragility behavior, J. Phys. Chem. 114 (2010) 14815–14820.
[20] R. Casalini, C.M. Ronald, Pressure evolution of the excess wing in a type-B glass former, Phys. Rev. Lett. 91 (2003) 015702–015704.
[21] R. Casalini, C.M. Ronald, Excess wing in the dielectric loss spectra of propyleneglycol oligomers at elevated pressure, Phys. Rev. B 91 (2004) 094202–094207.
[22] U. Schneider, R. Brand, P. Lunkenheimer, et al., Excess wing in the dielectric loss of glass formers: a Johari–Goldstein β relaxation? Phys. Rev. Lett. 84 (2000) 5560–5563.
[23] K.L. Ngai, P. Lunkenheimer, C. Leon, et al., Nature and properties of the Johari–Goldstein-relaxation in the equilibrium liquid state of a class of glass-formers, J. Chem. Phys. 115 (2001) 1405–1413.
[24] L.S. Shamblin, B.C. Hancock, Y. Dupuis, et al., Interpretation of relaxation time constants for amorphous pharmaceutical systems, J. Pharm. Sci. 89 (2000) 417–427.
[25] Z. Wojnarowska, L. Hawelek, M. Paluch, et al., Molecular dynamics at ambiet and elevated pressure of the amorphous pharmaceutical: nonivamide (pelargonic acid vanillylamide), J. Chem. Phys. 134 (2011) 044517.
[26] Z. Wojnarowska, K. Adrjanowicz, K. Kaminski, et al., Effect of pressure on tautomers' equilibrium in supercooled glibenclamide drug: analysis of fragility behavior, J. Phys. Chem. B 114 (2010) 14815–14820.
[27] Z. Wojnarowska, K. Grzybowska, L. Hawelek, et al., Molecular dynamics, physical stability and solubility advantage from amorphous indapamide drug, Mol. Pharm. 10 (2013) 3612–3627.
[28] C.A. Angell, Structural instability and relaxation in liquid and glassy phases near the fragile liquid limit, J. Non-Cryst. Solids 102 (1988) 205–221.
[29] R. Böhmer, K.L. Ngai, C.A. Angell, et al., Nonexponential relaxations in strong and fragile glass formers, J. Chem. Phys. 99 (1993) 4201–4209.
[30] T. Shibata, H. Igawa, T. Hyun Kim, et al., Glass transition dynamics of anti-inflammatory ketoprofen studied by Raman scattering and terahertz time-domain spectroscopy, J. Mol. Struct. 1062 (2014) 185–188.
[31] K. Pajula, M. Taskinen, V.P. Lehto, et al., Predicting the formation and stability of amorphous small molecule binary mixtures from computationally determined Flory–Huggins interaction parameter and phase diagram, Mol. Pham. 7 (2010) 795–804.
[32] K. Pajula, V.P. Lehto, J. Ketolainen, et al., Computational approach for fast screening of small molecular candidates to inhibit crystallization in amorphous drugs, Mol. Pham. 9 (2012) 2844–2855.